

**$\beta$ -decay of the neutron-rich nucleus  $^{18}\text{N}$** 

Z. H. Li, Y. L. Ye, H. Hua,\* D. X. Jiang, Y. M. Zhang, F. R. Xu, Q. Y. Hu, G. L. Zhang,  
Z. Q. Chen, T. Zheng, C. E. Wu, J. L. Lou, X. Q. Li, D. Y. Pang, S. Wang, and C. Li  
*School of Physics and MOE Key Laboratory of Heavy Ion Physics, Peking University, Beijing 100871, China*

H. S. Xu, Z. Y. Sun, L. M. Duan, Z. G. Hu, R. J. Hu, H. G. Xu, R. S. Mao, Y. Wang, X. H. Yuan,  
H. Gao, L. J. Wu, H. R. Qi, T. H. Huang, F. Fu, F. Jia, Q. Gao, X. L. Ding, J. L. Han, and X. Y. Zhang  
*Institute of Modern Physics, Chinese Academy of Sciences, Lanzhou 730000, China*

(Received 2 September 2005; published 30 December 2005)

The  $\beta$ -decay of  $^{18}\text{N}$  has been studied using  $\beta$ - $n$  and  $\beta$ - $\gamma$  coincidence methods. The  $^{18}\text{N}$  ions were produced by the fragmentation of the  $E/A = 68.8$  MeV  $^{22}\text{Ne}$  beam on a thick beryllium target. A newly constructed neutron detector system with wide energy detection range and low-energy detection threshold was used. The  $619 \pm 2$  ms half-life of the  $^{18}\text{N}$   $\beta$ -decay was found to be in very good agreement with the previous measurements. Transitions to 11  $\beta$ -delayed neutron emitting states in  $^{18}\text{O}$  have been observed with a total branching ratio of  $6.98 \pm 1.46\%$ . The Gamow-Teller  $\beta$ -decay strengths of  $^{18}\text{N}$  to these levels were deduced and compared with the shell model calculations. The intensities of the strong  $\gamma$ -ray transitions in  $^{18}\text{O}$  were found to be consistent with recent work.

DOI: [10.1103/PhysRevC.72.064327](https://doi.org/10.1103/PhysRevC.72.064327)

PACS number(s): 21.10.Pc, 23.40.-s, 23.90.+w, 27.20.+n

**I. INTRODUCTION**

For light neutron-rich nuclei, their  $\beta$ -decays are often characterized by the large decay energies (10~20 MeV), which will lead to the population of excited states with a wide excitation range, in particular particle unbound states, in the daughter nuclei. As a result, delayed neutrons or other particles may be emitted following the emission of  $\beta$ -rays. Such a complex decay scheme yields a great deal of information on  $\beta$ -decay properties of the neutron-rich mother nucleus and nuclear structures of the daughter nucleus, which provides a stringent test of the validity of structure models, such as the shell model. To get an unambiguous and precise determination of the complex decay scheme, as well as the information about the quantum state of the mother nucleus and states in the daughter nucleus, the coincidence measurements of the delayed neutrons or other particles with the  $\beta$ -rays are usually necessary.

We present here the spectroscopy of  $\beta$ -decay of the neutron-rich nucleus  $^{18}\text{N}$  using  $\beta$ - $n$  and  $\beta$ - $\gamma$  coincidence methods. The  $\beta$ -decay of nucleus  $^{18}\text{N}$  has been studied extensively [1–8] since it was first observed by Chase *et al.* [1] in 1964, and the spectroscopy of the daughter nucleus  $^{18}\text{O}$  has been established quite well via numerous studies [2–5,9]. Since the  $\beta$ -decay energy of  $^{18}\text{N}$  is 13.899 MeV, which lies above the alpha threshold at  $S_\alpha = 6.227$  MeV and the neutron threshold at  $S_n = 8.044$  MeV, delayed emissions of neutrons or alpha particles can occur. The total branching ratio to  $\alpha$ -emitting states has been found to be  $12.2 \pm 0.6\%$  by Zhao *et al.* [4] and a  $\beta$ -delayed neutron emission probability ( $P_n$ ) of  $14.3 \pm 2.0\%$  has been measured by Reeder *et al.* [6]. Among these measurements, one interesting feature is that a broad alpha group was observed at an excitation energy of 9.00 MeV with a width of about 500 keV [4,5]. In a recent work by Scheller

*et al.* [2], an attempt was made to measure the energy spectrum of delayed neutrons, and nine neutron peaks were observed at an energy from 0.99 to 3.26 MeV with a total branching ratio of  $2.2 \pm 0.4\%$ , which only accounted for a small part of total neutron-emission probability ( $P_n$ ) of  $14.3 \pm 2.0\%$  by Reeder [6]. In Ref. [2], the neutron detection threshold prohibited detection of the delayed neutrons of  $\leq 800$  keV resulting in a lesser value for the total branching ratio of  $^{18}\text{N}$  to neutron emitting states in  $^{18}\text{O}$ . Thus the missing  $\sim 12\%$  branching ratio is likely to proceed to states in  $^{18}\text{O}$  between 8.044 MeV (neutron threshold) and  $\sim 9.0$  MeV (low-energy neutron detection threshold in the  $^{18}\text{N}$  experiment of Ref. [2]).

Based on the above considerations, the present work focused on the low energy spectra of delayed neutrons from the  $\beta$ -decay of  $^{18}\text{N}$ . One recently constructed neutron detector system, which is designed for the study of  $\beta$ -delayed neutron emitting nuclei with wide energy range and low-energy detection threshold, was used and two missing branches to the neutron emitting states in  $^{18}\text{O}$  were observed.

**II. EXPERIMENT**

The present experiment was performed at the Institute of Modern Physics (IMP), Lanzhou, China. The primary beam for the experiment was 68.8 MeV per nucleon  $^{22}\text{Ne}$  ions produced by HIRFL, which impinged on a  $^9\text{Be}$  target with a thickness of 292.5 mg/cm<sup>2</sup>. The  $^{18}\text{N}$  fragments were collected, separated, and purified using the Radioactive Ion Beam Line in Lanzhou (RIBLL) [10]. The present experimental setup is shown in Fig. 1. The  $^{18}\text{N}$  beam passed through a thin aluminum window (10  $\mu\text{m}$  thick) which separated the vacuum of the beam line from the air. Before the  $^{18}\text{N}$  beam was finally stopped in a thin plastic scintillation detector, referred to as the implantation detector (NE102, 4.0 cm  $\times$  5.0 cm  $\times$  3.0 mm thick), it also passed an energy degrader (whose thickness was adjustable) and a silicon surface-barrier  $\Delta E$  detector (325  $\mu\text{m}$  thick,

\*Corresponding author. Email address: [Hhua@hep.pku.edu.cn](mailto:Hhua@hep.pku.edu.cn)

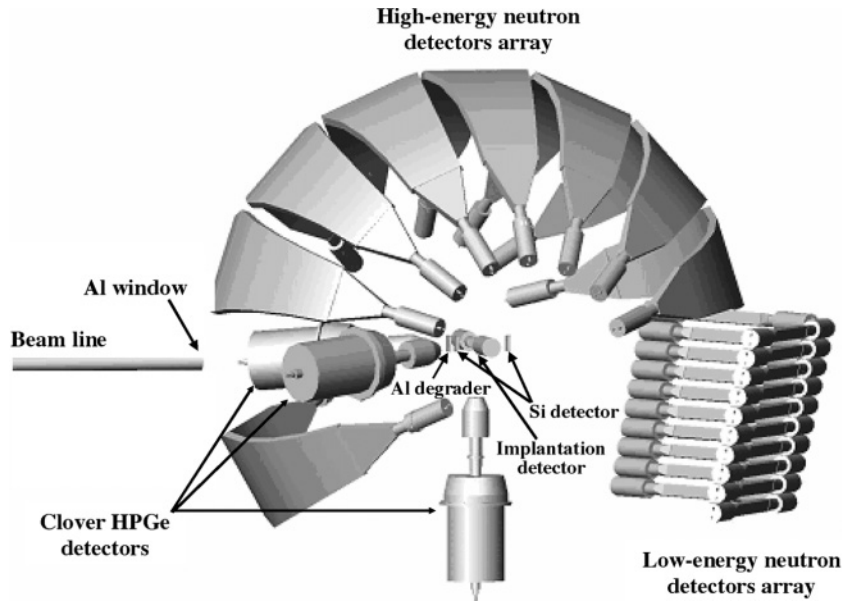


FIG. 1. Experimental setup for the  $\beta$ -decay measurement of  $^{18}\text{N}$ .

2000 mm<sup>2</sup> area) which, in combination with the time of flight measurement, was used for on-line monitoring of the purity of the  $^{18}\text{N}$  beam. The  $\Delta E$  detector also allowed us to determine the exact number of  $^{18}\text{N}$  ions deposited in the implantation detector. To verify that the  $^{18}\text{N}$  ions were indeed stopped in the implantation detector, a silicon surface-barrier veto detector (325  $\mu\text{m}$  thick, 2000 mm<sup>2</sup> area) was placed behind the implantation detector. During the experiment, the  $^{18}\text{N}$  beam had an intensity of about  $3.0 \times 10^3$  particles per second with an average beam purity of 95%. The main impurity was  $^{20}\text{O}$  ( $\sim 5\%$ ).

The  $\beta$ -rays from the decay of  $^{18}\text{N}$  were detected by the implantation detector which was optically coupled from two ends to two photomultiplier tubes (52 mm diameter EMI-9214B). The mean-time of these signals from the implantation detector served as the start for the neutron time-of-flight measurement. Delayed  $\gamma$ -rays were detected by three clover high-purity germanium (HPGe) placed about 20 cm, 35 cm, and 40 cm away from the implantation detector, respectively. All these clover HPGe detectors were calibrated using a standard  $^{152}\text{Eu}$   $\gamma$ -ray source.

Delayed neutrons from the  $\beta$ -decay of  $^{18}\text{N}$  were measured by a plastic scintillators (BC408) detection system. To cover a wide energy range of delayed neutrons and have a low-energy neutron detection threshold, two different plastic scintillator arrays were used: one for the high energies and the other for low energies. The detector array for high-energy neutron detection consisted of eight identical plastic scintillators [11]. To ensure that the neutrons had a uniform flight path, each of them (157 cm in length, 40 cm in width at the center, and 20 cm in width at both ends, 2.5 cm in thickness) was bent to have a 1 m radius of curvature. Two photomultiplier tubes (52 mm diameter EMI-9214B) were attached at both ends of the scintillator via light guides. The mean-time of these signals was used as the stop for the neutron time-of-flight measurement. The total solid angle of this detector array is approximately 30% of  $4\pi$  sr. The other detector array, used for low-energy neutron detection, consisted of 20 short plastic

scintillators (40.0 cm in length, 5.0 cm in width, 2.5 cm in thickness). The small size of these scintillators improved the light collection efficiency and led to high light transmission to photomultiplier tubes (52 mm diameter EMI-9214B) resulting in a low energy threshold. This detector array was located about 120 cm away from the implantation detector and covered a total solid angle of 2.2% of  $4\pi$  sr.

The neutron detection efficiencies of the neutron detector system were calibrated using the delayed neutron spectrum observed in the  $\beta$ -decay of  $^{17}\text{N}$ , which is known to be accompanied by delayed neutron emissions with the energies of  $382.8 \pm 0.9$  keV,  $1170.9 \pm 0.8$  keV, and  $1700.3 \pm 1.7$  keV with respective branching ratios of  $(38.0 \pm 1.3)\%$ ,  $(50.1 \pm 1.3)\%$ , and  $(6.9 \pm 0.5)\%$ . The absolute detection efficiency as a function of the neutron energy was calculated from the observed intensities of these three neutron peaks, their well-known branching ratios, and the sum of  $^{17}\text{N}$   $\beta$ -decays. Measured detection efficiencies for the low-energy neutron detector array are shown in Fig. 2. To extend the efficiency curve to higher energy, Monte Carlo calculations using the KSUEFF [12] program have been made. The results are also shown in Fig. 2. It has been shown in Ref. [12] that the KSUEFF program calculations are reliable to within 10% for neutron energy above 1.0 MeV. For the neutron energy below 1.0 MeV, because of the quick change of the detection efficiency curve and large statistical uncertainties of the experimental data near the detection threshold, the total uncertainties of the efficiencies for the energy region 0.5–1.0 MeV were expected to be about 20%. For the high-energy detector array, to have more experimental data at high energy region, an Am/Be neutron source was also used to calibrate its neutron detection efficiencies [11].

To enable the measurement of the  $\beta$ -decay of  $^{18}\text{N}$  with no interference from the direct beam, the cyclotron was cycled on and off at periodic intervals. During the experiment, since the half-life of  $624 \pm 12$  ms was found for  $^{18}\text{N}$  in the previous research [3], both the durations of beam-on and beam-off periods were chosen to be 2.0 s.

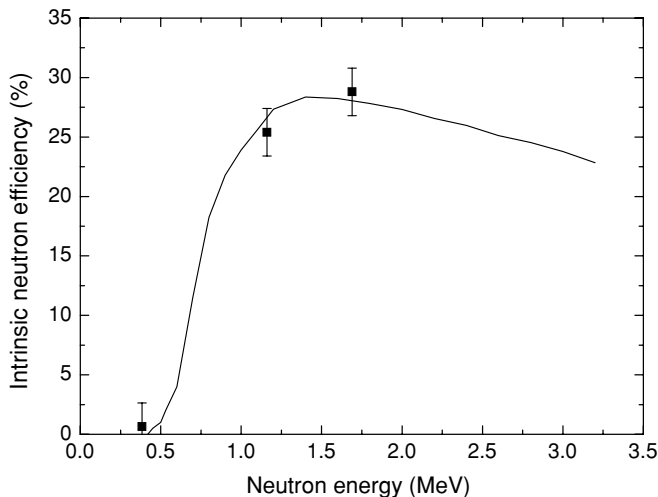


FIG. 2. Neutron efficiency as a function of neutron energy for the low-energy neutron detector array. The solid line represents the Monte Carlo calculations using the KSUEFF program.

### III. RESULTS AND DISCUSSION

The inclusive  $\beta$ -decay curve of  $^{18}\text{N}$ , obtained by measuring the time difference between the start of the beam off period and an event in the implantation detector during the same beam off period, was used for the determination of the half-life of  $^{18}\text{N}$ . The results are shown in Fig. 3(a). The decay spectrum was well fitted to a single exponential decay component plus a constant background. From the fit, a half-life of  $619 \pm 2$  ms was obtained. This value is in good agreement with the previous measured value of  $624 \pm 12$  ms [3]. The fit to the inclusive  $\beta$ -decay curve of  $^{18}\text{N}$  also resulted in a total measured decay event of  $6.01 \times 10^6$ .

The neutron time-of-flight spectrum measured by the low-energy neutron detector array is shown in Fig. 4. Time zero was deduced from the position of a prompt peak which was produced by relativistic electrons. Eleven  $\beta$ -delayed neutron peaks observed in Fig. 4 were fitted simultaneously with Gaussian line shapes and a cubic polynomial background,

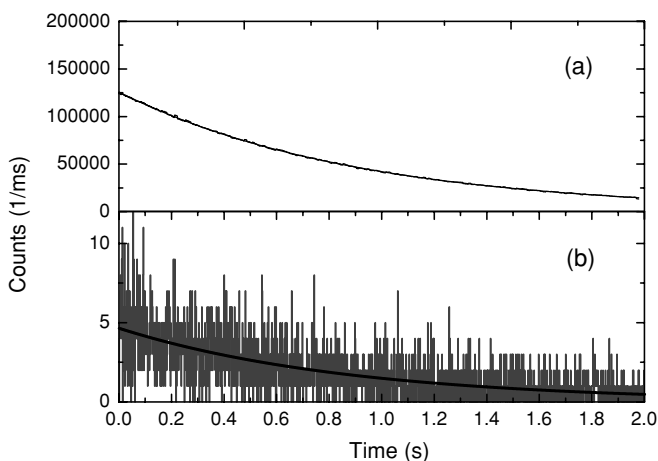


FIG. 3.  $\beta$ -decay curve of  $^{18}\text{N}$ ; (a) is the ungated decay curve and (b) is gated on the neutron group at 0.58 MeV.

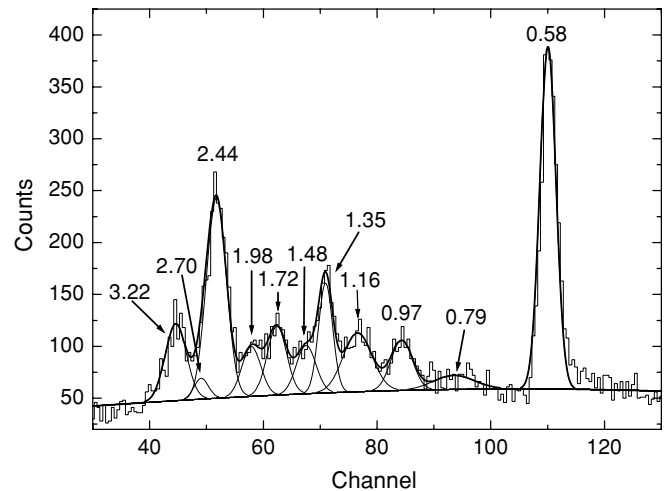


FIG. 4. Time-of-flight neutron spectrum of  $^{18}\text{N}$  obtained by the low-energy neutron detector array. The data were fitted with Gaussian line shapes and a cubic polynomial background. The neutron energies (lab) are given in keV.

using the program PEAKFITS. Resulting neutron lab energies are  $E_n(\text{lab}) = 3.22 \pm 0.05, 2.70 \pm 0.04, 2.44 \pm 0.04, 1.98 \pm 0.04, 1.72 \pm 0.03, 1.48 \pm 0.03, 1.35 \pm 0.03, 1.16 \pm 0.03, 0.97 \pm 0.02, 0.79 \pm 0.04, \text{ and } 0.58 \pm 0.02$  MeV. The fit shown in Fig. 4 represents a compromise between a flat background and a background with the maximum curvature allowed by a fit to the data. This uncertainty does not change the energies within the quoted error. The influence of the background on the neutron intensity has been estimated to be 10%. In the neutron time-of-flight spectrum measured by high-energy neutron detector array, nine neutron peaks at energies from 0.97 to 3.22 MeV were seen due to its high neutron detection threshold. The positions of the nine neutron peaks are in excellent agreement with that measured by the low-energy neutron detector array. No neutron peak was found at an energy region above 3.22 MeV in the high-energy spectrum.

After accounting for the recoil energy of the final nucleus and converting the neutron energy to the center-of-mass system, the excited states in  $^{18}\text{O}$  populated from the  $\beta$ -decays of  $^{18}\text{N}$  were obtained. The absolute branching ratios to neutron emitting states were calculated from the neutron yields at each energy, total neutron detection efficiency, and the sum of the  $\beta$ -decays. The total branching ratio of  $^{18}\text{N}$  to these 11 neutron unbound levels is  $6.98 \pm 1.46\%$ . The results from the present experiment are summarized in Table I. The  $\log ft$  values for the observed transitions, calculated from the half-life of  $^{18}\text{N}$  and the branching ratios, and Gamow-Teller decay strengths [ $B(\text{GT})$ ] are also listed in Table I. These experimentally derived  $\log ft$  values suggest that all decays are allowed transitions and limit the spins of observed levels in  $^{18}\text{O}$  to  $J^\pi = (0-2)^-$ .

Nine neutron groups with energies from 0.99 MeV to 3.26 MeV observed in this experiment are within the error in good agreement with the measurements published by Scheller *et al.* [2]. Presently the measured total branching ratio of  $1.66 \pm 0.28\%$  to these nine neutron unbound states is consistent with the previous result of  $2.2 \pm 0.4\%$  [2]. In Ref. [2], the levels at  $E_x = 8.521$  and  $8.660$  MeV were regarded

TABLE I. Summary of the experimental results for the  $\beta$ -delayed neutron decay of  $^{18}\text{N}$ . All energies are given in MeV.

$E_n(\text{lab})$	$E_x(^{18}\text{O})$	BR(%)	$\log ft$	$B(\text{GT})$	$J^\pi$
$3.22 \pm 0.05$	$11.45 \pm 0.05$	$0.23 \pm 0.03$	$4.91 \pm 0.06$	$0.075 \pm 0.010$	$(0-2)^-$
$2.70 \pm 0.04$	$10.90 \pm 0.04$	$0.13 \pm 0.02$	$5.54 \pm 0.07$	$0.018 \pm 0.003$	$(0-2)^-$
$2.44 \pm 0.04$	$10.63 \pm 0.04$	$0.43 \pm 0.06$	$5.12 \pm 0.06$	$0.047 \pm 0.006$	$(0-2)^-$
$1.98 \pm 0.04$	$10.14 \pm 0.04$	$0.11 \pm 0.03$	$5.96 \pm 0.12$	$0.007 \pm 0.002$	$(0-2)^-$
$1.72 \pm 0.03$	$9.89 \pm 0.03$	$0.18 \pm 0.02$	$5.86 \pm 0.05$	$0.009 \pm 0.001$	$(0-2)^-$
$1.48 \pm 0.03$	$9.61 \pm 0.03$	$0.05 \pm 0.02$	$6.51 \pm 0.17$	$0.002 \pm 0.001$	$(0-2)^-$
$1.35 \pm 0.03$	$9.47 \pm 0.03$	$0.24 \pm 0.04$	$5.90 \pm 0.07$	$0.008 \pm 0.001$	$(0-2)^-$
$1.16 \pm 0.03$	$9.28 \pm 0.03$	$0.18 \pm 0.03$	$6.11 \pm 0.07$	$0.005 \pm 0.001$	$(0-2)^-$
$0.97 \pm 0.02$	$9.07 \pm 0.02$	$0.11 \pm 0.03$	$6.41 \pm 0.12$	$0.002 \pm 0.001$	$(0-2)^-$
$0.79 \pm 0.04$	$8.89 \pm 0.04$	$0.28 \pm 0.06$	$6.08 \pm 0.09$	$0.005 \pm 0.001$	$(0-2)^-$
$0.58 \pm 0.02$	$8.66 \pm 0.02$	$5.04 \pm 1.12$	$4.87 \pm 0.10$	$0.083 \pm 0.018$	$(0-2)^-$
Total		$6.98 \pm 1.46$			

as promising candidates to have delayed-neutron emissions, since both states are the only known levels in the relevant excitation range which have not been observed in  $\alpha$ -induced reactions on  $^{14}\text{C}$  [13] as expected for a state with unnatural parity. This unnatural parity for these two states is also strongly suggested by the study of the  $^{16}\text{O}(t,p)$  reaction [14]. Our results confirmed this prediction and indicated that the level at  $E_x = 8.66$  MeV has a large  $\beta$ -decay branching ratio of  $5.04 \pm 1.12\%$ . No neutron peak related to  $E_x = 8.521$  MeV was observed in the present experiment. The other presently observed neutron emitting level at  $E_x = 8.89$  MeV was also seen in the  $^{16}\text{O}(t,p)$  reaction [14]. This state may also have alpha emission, which was discussed by Zhao *et al.* [4]. The missing branching of  $\sim 7.3\%$  seems to result from one or several states in  $^{18}\text{O}$  with excitation energy between 8.044 and 8.50 MeV, where the corresponding neutron group is below the threshold of our neutron detector system. Figure 3(b) shows the  $\beta$ -decay spectrum gated on the neutron peak at  $E_n(\text{lab}) = 0.58$  MeV. The spectrum was fitted with a single exponential and the resulting half-life of  $610 \pm 23$  ms, which is consistent with the result from the inclusive  $\beta$ -decay spectrum and result reported in Ref. [3].

Theoretical calculations for  $\beta$ -decay of  $^{18}\text{N}$  were carried out to describe the transition from the initial decaying nucleus to possible final states in *spsdpf* model space with the computer code OXBASH [15]. The WB10 interaction, which is based on the WBT interaction [16], was used. It predicted a half-life of  $T_{1/2} = 623$  ms for the  $\beta$ -decay of  $^{18}\text{N}$ , which is in good agreement with the  $619 \pm 2$  ms measured here and result by Onless [3].  $\beta$ -decay of  $^{18}\text{N}$  to 15 neutron unbound states in  $^{18}\text{O}$  up to 11.54 MeV in excitation energy were predicted with a total branching ratio of 11.7%, which is in reasonable agreement with the experimental value of  $14.3 \pm 2.0\%$  [6]. The summed Gamow-Teller strength of the  $\beta$ -decay to these predicted neutron unbound states between 8.0 and 11.54 MeV in  $^{18}\text{O}$  was  $B(\text{GT}) = 0.488$  as compared to the total deduced  $B(\text{GT}) = 0.261 \pm 0.045$  in the present work. Here we assumed these neutron unbound states have a neutron width much larger than the alpha particle width. These theoretical  $B(\text{GT})$  values have included the  $(g_a/g_v)^2$  factor and have been multiplied by a factor of 0.6 to take into account the empirical quenching

observed for Gamow-Teller decay strength in *sd*-shell nuclei [17]. Figure 5 compares the experimental Gamow-Teller strengths with the calculations by the shell model. The figure shows the individual Gamow-Teller strengths for the excitation range in  $^{18}\text{O}$  observed in this work. The agreement between the shell model predictions and the detailed experimental strength distribution is very good for excitation energy above 10.5 MeV. For excitation energy below 10.5 MeV, theoretical calculations predicted two strong  $\beta^-$  transitions to the 9.71 and 10.41 MeV levels in  $^{18}\text{O}$ , which were not observed in this work and measurements by Scheller [2]. The newly observed strong  $\beta^-$  transition to the 8.66 MeV level in  $^{18}\text{O}$  was not predicted by the calculations. One of these two predicted two strong  $\beta^-$  transitions to the 9.71 and 10.41 MeV levels in  $^{18}\text{O}$  may be associated with the newly observed strong  $\beta^-$  transition to the 8.66 MeV level. The discrepancy between experimental results and calculations might be ascribed to the determination of effective interactions. The newly obtained information for  $^{18}\text{N}$   $\beta$ -delayed neutron decay should be helpful in the effort of improving the nuclear structure model and understanding

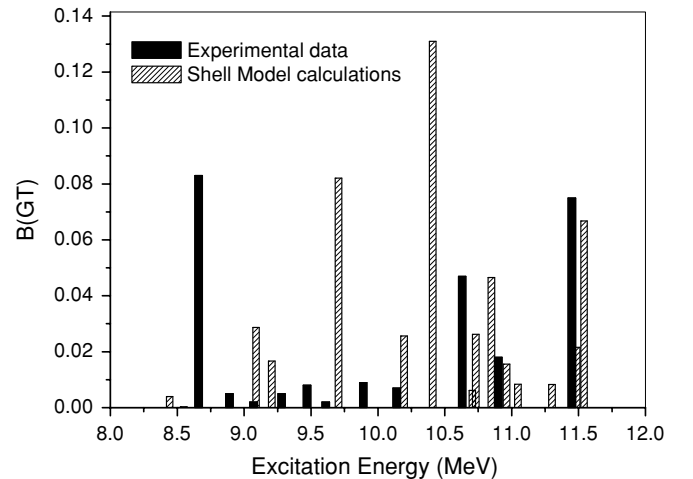


FIG. 5. Comparisons of shell model predictions to observed individual Gamow-Teller strengths for the  $\beta$ -decay of  $^{18}\text{N}$  to neutron unbound states in  $^{18}\text{O}$ .

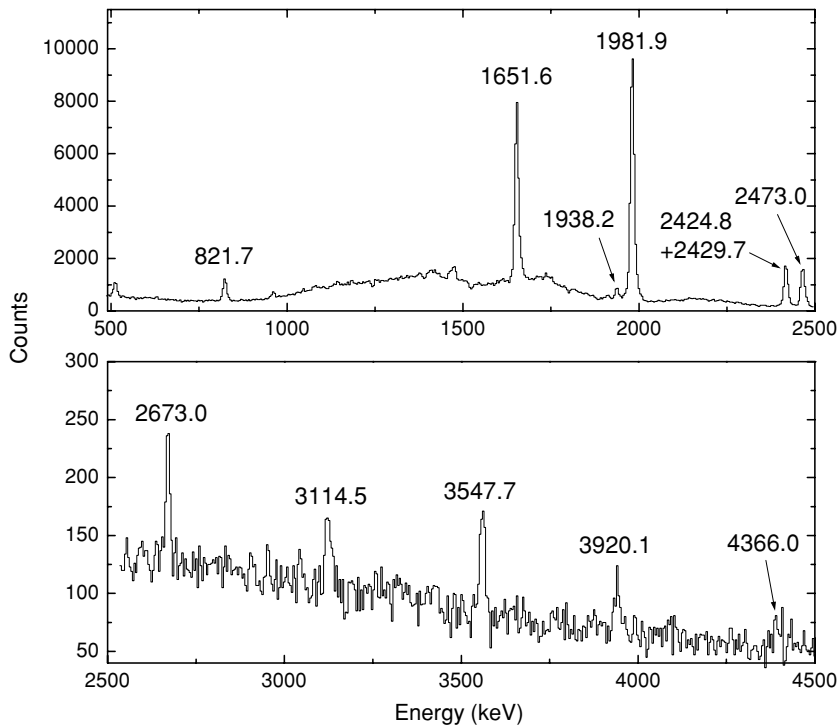


FIG. 6. The  $\gamma$ -ray spectra observed in coincidence with  $\beta$ -rays. The spectra are shown in two segments. The  $\gamma$ -ray energies (lab) are given in keV.

effective interactions better. One thing necessary to mention is that here we did not include the contribution coming from the observed broad alpha group at the  $E_x \sim 9$  MeV [4]. The Gamow-Teller strength of the  $\beta$ -decay to this state was deduced to be  $B(\text{GT}) = 0.06$  [4].

The  $\gamma$ -rays following the  $\beta$ -decay of  $^{18}\text{N}$  have been studied extensively. Figure 6 shows the  $\gamma$ -ray spectra measured in coincidence with  $\beta$ -rays in the present work. Many peaks were found and identified to be the known transitions in the daughter nucleus  $^{18}\text{O}$ . From the work of Olness *et al.* [3], the 1652 keV transition in  $^{18}\text{O}$  has a relative  $\gamma$  branching ratio of  $60.48 \pm 1.80\%$ . In the present work, the 1652 keV transition in  $^{18}\text{O}$  was found to have an absolute branching ratio of  $42.5 \pm 3.9\%$  which results in an absolute branching ratio for all  $\gamma$ -ray emission of  $70.3 \pm 6.8\%$ . This value is consistent with the measurement of  $76.7 \pm 7.2(\text{stat}) \pm 5.8(\text{norm})\%$  by France *et al.* [8]. It is also in good agreement with the result of  $70.9 \pm 2.1\%$  which was deduced from the total branching ratio for non- $\gamma$ -ray decay.

#### IV. CONCLUSION

The  $\beta$ -decay of  $^{18}\text{N}$  has been studied using  $\beta$ - $n$  and  $\beta$ - $\gamma$  coincidence methods. A newly constructed neutron detector system with wide energy range and low-energy detection threshold was used. The  $619 \pm 2$  ms half-life of  $^{18}\text{N}$  was found to be in very good agreement with the previous measurements.

Transitions to 11  $\beta$ -delayed neutron emitting states in  $^{18}\text{O}$  have been observed with a total branching ratio of  $6.98 \pm 1.46\%$ . Two delayed-neutron emitting states observed for the first time were found to have a large branching ratio of  $5.32 \pm 1.18\%$ . The missing branching of  $\sim 7.3\%$  seems to result from one or several states in  $^{18}\text{O}$  with an excitation energy between 8.044 and 8.50 MeV, where the corresponding neutron group is below the threshold of our neutron detectors system. Shell model calculations performed for the  $\beta$ -decay of  $^{18}\text{N}$  are compared with experimental results. The discrepancy of detailed Gamow-Teller decay strength between experimental results and calculations indicated that a better determination of effective interactions might be needed. To get a deeper understanding of  $\beta$ -decay properties of  $^{18}\text{N}$ , further experimental and theoretical work is needed. The intensities of the strong  $\gamma$ -ray transitions of  $^{18}\text{O}$  observed in present experiment were found to be consistent with recent work.

#### ACKNOWLEDGMENTS

The authors wish to thank the staffs in the HIRFL and RIBLL at the Institute of Modern Physics (IMP), Lanzhou, China. This work is support by the National Natural Science Foundation of China (10475004, 10405001, 10221003) and the Major State Basic Research Development Program (G2000077400).

- [1] L. F. Chase, Jr., H. A. Grench, R. E. McDonald, and F. J. Vaughn, Phys. Rev. Lett. **13**, 665 (1964).  
 [2] K. W. Scheller, J. Görres, J. G. Ross, M. Wiescher, R. Harkewicz, D. J. Morrissey, B. M. Sherrill, M. Steiner, N. A. Orr, and J. A. Winger, Phys. Rev. C **49**, 46 (1994).

- [3] J. W. Olness, E. K. Warburton, D. E. Alburger, C. J. Lister, and D. J. Millener, Nucl. Phys. **A373**, 13 (1982).  
 [4] Z. Zhao, M. Gai, B. J. Lund, S. L. Rugari, D. Mikolas, B. A. Brown, J. A. Nolen, and M. Samuel, Phys. Rev. C **39**, 1985 (1989).

- [5] F. Ajzenberg-Selove, Nucl. Phys. **A475**, 1 (1987).
- [6] P. L. Reeder, R. A. Warner, W. K. Hensley, D. J. Vieira, and J. M. Wouters, Phys. Rev. C **44**, 1435 (1991).
- [7] W.-T. Chou, E. K. Warburton, and B. A. Brown, Phys. Rev. C **47**, 163 (1993).
- [8] R. H. France III, Z. Zhao, and M. Gai, Phys. Rev. C **68**, 057302 (2003).
- [9] D. R. Tilley, H. R. Weller, C. M. Cheves, and R. M. Chasteler, Nucl. Phys. **A595**, 1 (1995), and references therein.
- [10] Z. Sun, W. L. Zhan, Z. Y. Guo, G. Xiao, J. X. Li, Nucl. Instrum. Methods Phys. Res. A **503**, 496 (2003).
- [11] Q. Y. Hu, Y. L. Ye, Z. H. Li, X. Q. Li, D. X. Jiang, T. Zheng, Q. J. Wang, H. Hua, C. E. Wu, Z. Q. Chen, J. Ying, D. Y. Pang, G. L. Zhang, and J. Wang, IEEE Trans. Nucl. Sci. **52**, 473 (2005).
- [12] R. A. Cecil, B. D. Anderson, and R. Madey, Nucl. Instrum. Methods **161**, 439 (1979).
- [13] J. K. Bair, J. L. C. Ford, Jr., and C. M. Jones, Phys. Rev. **144**, 799 (1966).
- [14] M. E. Cobern, L. C. Bland, H. T. Fortune, G. E. Moore, S. Mordechai, and R. Middleton, Phys. Rev. C **23**, 2387 (1981).
- [15] B. A. Brown, A. Etchegoyen, and W. D. M. Rae, computer code OXBASH, MSU-NSCL report 524 (1988).
- [16] E. K. Warburton and B. A. Brown, Phys. Rev. C **46**, 923 (1992).
- [17] B. A. Brown and B. H. Wildenthal, Annu. Rev. Part. Sci. **38**, 29 (1988).